

The distance between exceptional points and diabolic points and its implication for the response strength of non-Hermitian systems

Jan Wiersig

Institut für Physik, Otto-von-Guericke-Universität Magdeburg, Postfach 4120, D-39016 Magdeburg, Germany^{*}

(Dated: June 1, 2022)

Exceptional points are non-Hermitian degeneracies in open quantum and wave systems at which not only eigenenergies but also the corresponding eigenstates coalesce. This is in strong contrast to degeneracies known from conservative systems, so-called diabolic points, at which only eigenenergies degenerate. Here we connect these two kinds of degeneracies by introducing the concept of the distance of a given exceptional point in matrix space to the set of diabolic points. We prove that this distance determines an upper bound for the response strength of a non-Hermitian system with this exceptional point. A small distance therefore implies a weak spectral response to perturbations and a weak intensity response to excitations. This finding has profound consequences for physical realizations of exceptional points that rely on perturbing a diabolic point. Moreover, we exploit this concept to analyze the limitations of the spectral response strength in passive systems. A number of optical and photonics systems are investigated to illustrate the theory.

I. INTRODUCTION

Open quantum and wave dynamics and its exotic degeneracies, so-called exceptional points (EPs), have gained substantial attention in recent years, primarily in optics and photonics [1, 2]. At an EP of order n exactly n eigenenergies (eigenfrequencies) and the corresponding energy eigenstates (modes) coalesce [1, 3–6]. This is very different from a conventional degeneracy, known as diabolic point (DP) [7], at which only the eigenenergies coalesce. For an EP to exist, the Hamiltonian \hat{H} has to be not only non-Hermitian, $\hat{H} \neq \hat{H}^\dagger$, but also nonnormal, i.e., $[\hat{H}, \hat{H}^\dagger] \neq 0$.

EPs have been observed in numerous experiments in diverse physical systems [8–19]. Several applications of EPs have been suggested, such as unidirectional lasing operation [13], orbital angular momentum microlasers [20], sources of circularly polarized light [21], topological energy transfer between states [22, 23], loss-induced suppression of lasing [24], mode discrimination in multimode laser cavities [25], and sensors with enhanced response [26–32].

The sensing applications of EPs (a review can be found in Ref. [33]) rely on the strong spectral response to perturbations. A system with an EP_n shows an energy (frequency) splitting proportional to the n th root of the perturbation strength ε [3], which for sufficiently small perturbations is larger than the linear scaling near a DP. In Ref. [34] it was shown that the spectral response to perturbations can be characterized by the so-called spectral response strength ξ . A large ξ does not only indicate a large spectral response to generic perturbations but also a large intensity response to excitations and a large dynamic response to an initial deviation from the EP eigenstate.

One convenient way to create an EP is to start with a DP and to perturb it appropriately [5, 35, 36]. For instance, optical modes of ideal whispering-gallery microcavities naturally come as degenerate pairs of clockwise and counterclockwise traveling waves. Such a DP can be converted into an EP by

weak local perturbations [13, 37, 38] or weak boundary deformations [39, 40] without adding extra parasitic radiation losses. Another example is the efficient transfer of excitations between energy levels, which is usually done as rapid adiabatic passage through a DP. Weakly perturbing it maps this scheme to one based on encircling an EP, which has been demonstrated experimentally using microwave waveguides [41]. Another example where EPs originating from perturbed DPs have been observed are systems of interacting fermions [42]. Finally, DPs naturally appear in periodic systems as Dirac or Weyl points in the band structure. These can too be used to create EPs, which has been done for photonic crystals [43–46], Dirac superconductors [47], optically biaxial crystals [14], and for a Hubbard model [48].

The aim of the present paper is to introduce the concept of the distance Δ between a given EP_n and the set of DPs of the same order n . This distance quantifies the difference of the $n \times n$ Hamiltonians exhibiting these two different kinds of degeneracies. We show that Δ is an upper bound for the spectral response strength ξ associated with the EP; see Fig. 1. The important conclusion is that EPs generated by a small perturbation of a DP necessarily exhibit only a weak spectral response to perturbations, which renders a number of applications difficult.

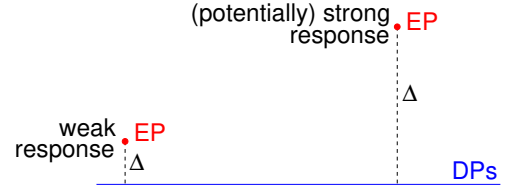


FIG. 1. Sketch of the distance Δ (dashed lines) between a given exceptional point (EP) and the set of diabolic points of the same order (DPs, solid line) in matrix space. A key result of this paper is that while a system with an EP which is close to a DP shows only a weak spectral response to perturbations, a system having an EP with a large distance can exhibit a strong spectral response to perturbations.

The outline of the paper is as follows. Section II provides some mathematical preliminaries that are needed for the sub-

^{*} jan.wiersig@ovgu.de

sequent sections. Section III introduces the notion of the distance between a given Hamiltonian and the set of diabolic points. In Sec. IV the relation to the spectral response strength is explored. Section V investigates the relevant aspects for passive systems. Various examples are considered in Sec. VI. A discussion and summary is given in Sec. VII.

II. MATRIX NORMS AND DISTANCES

The aim of this section is to review some aspects of linear algebra required in this article.

A. Matrix norms

A matrix norm $\|\hat{A}\|$ is defined as a mapping of a matrix \hat{A} to the nonnegative real numbers, see, e.g., Ref. [49], with the properties

$$\|\hat{A} + \hat{B}\| \leq \|\hat{A}\| + \|\hat{B}\| \text{ (triangle inequality),} \quad (1)$$

$$\|\alpha \hat{A}\| = |\alpha| \|\hat{A}\| \text{ (absolutely homogeneous),} \quad (2)$$

$$\|\hat{A}\| = 0 \text{ if and only if } \hat{A} = 0 \text{ (definite),} \quad (3)$$

$$\|\hat{A}\hat{B}\| \leq \|\hat{A}\| \|\hat{B}\| \text{ (submultiplicative),} \quad (4)$$

for all matrices \hat{A} and \hat{B} and $\alpha \in \mathbb{C}$. The nonnegativity of $\|\cdot\|$ follows from the first two items.

Important examples of matrix norms are the Frobenius norm

$$\|\hat{A}\|_{\text{F}} := \sqrt{\text{Tr}(\hat{A}^\dagger \hat{A})} \quad (5)$$

with the trace Tr and the spectral norm

$$\|\hat{A}\|_2 := \max_{\|\psi\|_2=1} \|\hat{A}\psi\|_2. \quad (6)$$

We adopt the common but slightly confusing notation $\|\cdot\|_2$ both for the spectral matrix norm [in the left-hand side (LHS) of Eq. (6)] and the vector 2-norm $\|\psi\|_2 = \sqrt{\langle \psi | \psi \rangle}$ of a vector $|\psi\rangle$ based on the usual inner product in complex vector space [in the right-hand side (RHS) of Eq. (6)]. Both matrix norms (5) and (6) share the important property of unitarily invariance, i.e.,

$$\|\hat{U} \hat{A} \hat{V}\| = \|\hat{A}\| \quad (7)$$

for all matrices \hat{A} and all unitary matrices \hat{U} and \hat{V} . Moreover, both matrix norms (5) and (6) are compatible with the vector 2-norm, i.e.,

$$\|\hat{A}\psi\|_2 \leq \|\hat{A}\| \|\psi\|_2 \quad (8)$$

for all matrices \hat{A} and vectors $|\psi\rangle$. The following inequality holds for all matrices \hat{A}

$$\|\hat{A}\|_2 \leq \|\hat{A}\|_{\text{F}}, \quad (9)$$

with equality for rank-1 matrices.

The calculation of the Frobenius norm (5) is particularly easy

$$\|\hat{A}\|_{\text{F}} = \sqrt{\sum_{ij} |A_{ij}|^2} \quad (10)$$

where A_{ij} are the matrix elements of \hat{A} in any orthonormal basis. Also beneficial for us is that the Frobenius norm can be derived from an inner product,

$$\|\hat{A}\|_{\text{F}}^2 = \langle \hat{A}, \hat{A} \rangle_{\text{F}}. \quad (11)$$

The inner product is the Frobenius inner product, see, e.g., Ref. [49], of two matrices \hat{A} and \hat{B} ,

$$\langle \hat{A}, \hat{B} \rangle_{\text{F}} := \text{Tr}(\hat{A}^\dagger \hat{B}). \quad (12)$$

B. Matrix distances

The distance between any two matrices \hat{A} and \hat{B} can be measured with the distance function (see, e.g., Ref. [50])

$$d(\hat{A}, \hat{B}) := \|\hat{A} - \hat{B}\|, \quad (13)$$

with arbitrary matrix norm. It is easy to show that this distance function fulfills the usual axioms of a metric:

$$d(\hat{A}, \hat{B}) = 0 \text{ if and only if } \hat{A} = \hat{B} \text{ (identity of indiscernibles)} \quad (14)$$

$$d(\hat{A}, \hat{B}) = d(\hat{B}, \hat{A}) \text{ (symmetry)} \quad (15)$$

$$d(\hat{A}, \hat{B}) \leq d(\hat{A}, \hat{C}) + d(\hat{C}, \hat{B}) \text{ (triangle inequality)} \quad (16)$$

$$d(\hat{A}, \hat{B}) \leq d(\hat{A}, \hat{C}) + d(\hat{C}, \hat{B}) \text{ (triangle inequality)} \quad (17)$$

for all matrices \hat{A} , \hat{B} , and \hat{C} . From these axioms one can deduce $d(\hat{A}, \hat{B}) \geq 0$.

It is important to mention that the assumed unitary invariance of the matrix norm (7) transfers to the distance function (13).

III. DISTANCE BETWEEN A GIVEN HAMILTONIAN AND THE SET OF DPS

In the mathematical literature several matrix nearness problems had been studied, as reviewed in Ref. [51]. For example, one asks the question of how close a given nonnormal matrix \hat{A} is to the set of normal matrices and which normal matrix \hat{B} is minimizing the distance function such as in Eq. (13). A rather difficult task is to find the nearest matrix having at least two equal eigenvalues; see, e.g., Ref. [52]. Our problem is related but simpler.

We consider an, in general, nonnormal $n \times n$ -matrix \hat{H} and a non-Hermitian but normal $n \times n$ -matrix $\hat{H}_{\text{DP}} = E_{\text{DP}} \mathbb{1}$ with a DP of order n with complex-valued eigenvalue E_{DP} and $n \times n$ -identity matrix $\mathbb{1}$. Note that \hat{H}_{DP} is in the above form in any orthonormal basis. Using the distance function (13) we define the distance between \hat{H} and a given DP by $d(\hat{H}, E_{\text{DP}} \mathbb{1})$. The

distance between \hat{H} and the set of DPs of order n is then given by

$$\Delta(\hat{H}) := \min\{d(\hat{H}, E_{\text{DP}}\mathbb{1}), E_{\text{DP}} \in \mathbb{C}\}. \quad (18)$$

Introducing the traceless part of the Hamiltonian

$$\hat{H}' := \hat{H} - \bar{E}\mathbb{1} \quad (19)$$

with the mean energy $\bar{E} := \text{Tr } \hat{H}/n \in \mathbb{C}$, we write

$$d(\hat{H}, E_{\text{DP}}\mathbb{1}) = \|\hat{H} - E_{\text{DP}}\mathbb{1}\| = \|\hat{H}' - (E_{\text{DP}} - \bar{E})\mathbb{1}\|. \quad (20)$$

We now choose the Frobenius norm and evaluate with Eq. (11)

$$\|\hat{H}' - (E_{\text{DP}} - \bar{E})\mathbb{1}\|_{\text{F}}^2 = \|\hat{H}'\|_{\text{F}}^2 + n|E_{\text{DP}} - \bar{E}|^2, \quad (21)$$

where we have exploited $\langle \mathbb{1}, \mathbb{1} \rangle_{\text{F}} = n$, $\langle \mathbb{1}, \hat{H}' \rangle_{\text{F}} = \text{Tr } \hat{H}' = 0$, and correspondingly $\langle \hat{H}', \mathbb{1} \rangle_{\text{F}} = 0$. Hence we get

$$d(\hat{H}, E_{\text{DP}}\mathbb{1}) = \sqrt{\|\hat{H}'\|_{\text{F}}^2 + n|E_{\text{DP}} - \bar{E}|^2}. \quad (22)$$

Clearly, this expression is minimal for $E_{\text{DP}} = \bar{E}$ and the minimizing $\hat{H}_{\text{DP}} = E_{\text{DP}}\mathbb{1}$ is unique. Plugging this into Eq. (18) gives the first result

$$\Delta(\hat{H}) = \|\hat{H}'\|_{\text{F}}. \quad (23)$$

As the Frobenius norm is unitarily invariant, we can evaluate the matrix norm in Eq. (23) in an orthonormal basis of our choice.

From Eq. (10) we can infer that the physical interpretation of the distance (23) is that of an Euclidean distance defined on an $n \times n$ complex matrix space. The matrix space is usually of higher dimension than the parameter space, i.e., the space spanned by the physical parameters relevant for a given system. But this disadvantage is outweighed by the geometric tools provided by linear algebra, such as norms and inner products.

A small distance $\Delta(\hat{H})$ means a minor change of the matrix elements of \hat{H} compared to \hat{H}_{DP} . This translates to a small detuning of the system's parameters away from the DP.

A. Hamiltonian without an EP

For a nonnormal Hamiltonian \hat{H} that does not have an EP, one can express the distance to the set of DPs in terms of the biorthogonal basis of the Hamiltonian

$$\hat{H}|R_j\rangle = E_j|R_j\rangle \text{ and } \langle L_j|\hat{H} = E_j\langle L_j| \quad (24)$$

with the right eigenstates $|R_j\rangle$ and the left eigenstates $|L_j\rangle$; see, e.g., Ref. [53]. With $\langle L_j|R_l\rangle = 0$ if $j \neq l$ and the normalization $\langle L_j|R_j\rangle = 1$ for all j , the biorthogonal expansion

$$\hat{H} = \sum_j E_j|R_j\rangle\langle L_j|, \quad (25)$$

and $\text{Tr}(|R_j\rangle\langle L_l|) = \langle L_l|R_j\rangle$ it is straightforward to show with Eq. (23) that

$$\Delta(\hat{H}) = \sqrt{\sum_{j,l} (E_j - \bar{E})^*(E_l - \bar{E})O_{lj}} \quad (26)$$

with the $n \times n$ matrix

$$O_{lj} := \langle R_j|R_l\rangle\langle L_l|L_j\rangle. \quad (27)$$

This matrix is known as the nonorthogonality overlap matrix [53–55]. Its diagonal elements are the Petermann factors of the eigenstates [56, 57], a measure of nonorthogonality. In Ref. [31] the expression $\|\hat{H}'\|_{\text{F}}$ (without relating it to a distance function) has been used to calculate the Petermann factors for the special case of $n = 2$.

From Eq. (26) we learn that the distance of the Hamiltonian \hat{H} to its nearest DP depends on the distance of its eigenvalues to the DP eigenvalue $E_{\text{DP}} = \bar{E}$ and the nonorthogonality of its eigenstates. It is to emphasize that we do not advocate the use of Eq. (26) for calculating $\Delta(\hat{H})$. It is much easier to evaluate directly Eq. (23). Moreover, Eq. (26) is not valid for \hat{H} having an EP. At the EP the Petermann factors diverge and the expansion (25) is not valid.

B. Hamiltonian with an EP

Next we consider the more interesting case of an $n \times n$ -Hamiltonian $\hat{H} = \hat{H}_{\text{EP}}$ having an EP of order n with complex-valued eigenvalue E_{EP} (frequency ω_{EP} for optical systems). It follows from $\bar{E} = E_{\text{EP}}$ that the traceless part of the Hamiltonian [Eq. (19)] equals the operator

$$\hat{N} := \hat{H}_{\text{EP}} - E_{\text{EP}}\mathbb{1}. \quad (28)$$

The matrix \hat{N} is nilpotent of index n , i.e., $\hat{N}^n = 0$ but $\hat{N}^{n-1} \neq 0$; see Ref. [34]. From Eq. (23) it follows for a Hamiltonian with an EP the important result

$$\Delta(\hat{H}_{\text{EP}}) = \|\hat{N}\|_{\text{F}}. \quad (29)$$

The distance of an EP to the set of DPs in Eq. (29) can be related to the Henrici's departure from normality [58]

$$\mathcal{D}(\hat{A}) := \sqrt{\|\hat{A}\|_{\text{F}}^2 - \sum_{j=1}^n |\lambda_j(\hat{A})|^2} \quad (30)$$

where $\lambda_j(\hat{A})$ are the eigenvalues of the matrix \hat{A} . Clearly, $\mathcal{D}(\hat{A}) \neq 0$ only if \hat{A} is nonnormal. In our case $\hat{A} = \hat{N}$ from Eq. (28) has only zero eigenvalues as the matrix is nilpotent. As a consequence, the distance of a given EP to the set of DPs in Eq. (29) can be expressed by the departure of \hat{N} from normality,

$$\Delta(\hat{H}_{\text{EP}}) = \mathcal{D}(\hat{N}). \quad (31)$$

It is known that Henrici's departure from normality is an upper bound for the distance of a matrix to the set of normal matrices [51]. The quantity $\Delta(\hat{H}_{\text{EP}})$ is therefore also an upper bound of the distance of the matrix \hat{H}_{EP} to the set of normal matrices.

From the physics perspective we can consider the departure of \hat{N} from normality and the distance of an EP to the set of DPs in many cases as a vague measure of the experimental effort in realizing the EP when starting at or near an DP. We come back to this point later when discussing some examples in Sec. VI.

IV. RELATION TO THE SPECTRAL RESPONSE STRENGTH

In Ref. [34] the spectral response strength of a system with an EP of order n has been determined to be

$$\xi = \|\hat{N}^{n-1}\|_2 = \|\hat{N}^{n-1}\|_{\text{F}}. \quad (32)$$

The spectral norm and the Frobenius norm give in this particular case the same result since \hat{N}^{n-1} has rank 1, which is a consequence of the nilpotency of \hat{N} . The spectral response strength is unitarily invariant. It describes the response of the system to perturbations,

$$\hat{H} = \hat{H}_0 + \varepsilon \hat{H}_1 \quad (33)$$

with $\hat{H}_0 = \hat{H}_{\text{EP}}$. The spectral response strength shows up as a factor in the bound of the eigenvalue splittings

$$|E_j - E_{\text{EP}}|^n \leq \varepsilon \|\hat{H}_1\|_2 \xi, \quad (34)$$

where higher orders in the perturbation strength ε are ignored. The scaling of the splittings $|E_j - E_{\text{EP}}|$ with the n th root of ε expresses the enhanced sensitivity of the EP with respect to perturbations. It is important to mention that ξ also bounds the intensity response to excitations [34]:

$$\|\psi\|_2^{\text{EP}} \leq P \frac{1}{|\hbar\omega - E_{\text{EP}}|^n} \xi, \quad (35)$$

where the vector $|\psi\rangle \propto e^{-i\omega t}$ is the long-time asymptotics of the equation of motion

$$i\hbar \frac{d}{dt} |\psi\rangle = \hat{H}_0 |\psi\rangle + e^{-i\omega t} P |p\rangle \quad (36)$$

with the excitation power $P \geq 0$, the excitation frequency $\omega \in \mathbb{R}$, and a generic excitation vector $|p\rangle$ normalized to unity.

Comparing Eq. (29) to Eq. (32) reveals that in the special case of an EP₂

$$\xi = \Delta(\hat{H}_{\text{EP}}) \text{ for } n = 2. \quad (37)$$

Hence the spectral response strength associated with the EP and its distance to the set of DPs in the Frobenius norm is exactly the same. This is different for higher-order EPs. With the submultiplicativity (4), we could use

$$\|\hat{N}^{n-1}\|_{\text{F}} \leq \|\hat{N}\|_{\text{F}}^{n-1} \quad (38)$$

to derive an upper bound for ξ determined by $\Delta(\hat{H}_{\text{EP}})$. However, a more stringent bound can be obtained by taking advantage of the nilpotency of \hat{N} . For a nilpotent matrix \hat{N} with index $n > 2$ holds [59]

$$\|\hat{N}^k\|_{\text{F}} \leq \gamma_{n,k} \|\hat{N}\|_{\text{F}}^k \quad (39)$$

with $k = 1, \dots, n-1$ and positive numbers $\gamma_{n,k}$ given by

$$\gamma_{n,k}^2 = \frac{(n-1)(n-2) \dots (n-k)}{(n-1)^k k!}. \quad (40)$$

For $k = n-1$ we get

$$\|\hat{N}^{n-1}\|_{\text{F}} \leq (n-1)^{-\frac{n-1}{2}} \|\hat{N}\|_{\text{F}}^{n-1}. \quad (41)$$

This inequality, being valid for \hat{N} being nilpotent of index $n > 2$, provides a much sharper bound than the inequality (38). Combining the inequality (41) with Eqs. (29) and (32) we arrive at our next crucial result

$$\xi \leq \left(\frac{\Delta(\hat{H}_{\text{EP}})}{\sqrt{n-1}} \right)^{n-1}. \quad (42)$$

The spectral response strength associated with the EP is therefore bounded by its distance to the set of DPs in the Frobenius norm. The important implication is: if the EP is generated by a small perturbation of a DP then the spectral response strength of the resulting EP is weak. Clearly, this has a profound impact on applications such as EP-based sensing. Note that small perturbation means here small compared to a perturbation needed to create another EP (of the same order) out of a DP. That one has a potentially larger spectral response strength than the first EP, as illustrated in Fig. 1.

Equation (42) can be also seen as an estimate for the spectral response strength ξ . The calculation of $\Delta(\hat{H}_{\text{EP}})$ is considerably simpler and faster.

In the context of the response strength of a system with an EP the physical interpretation of the nearest DP is that of a reference. To discuss this, consider the spectral response to a perturbation $\varepsilon \hat{H}_1$. For EP-based sensors it is common to compare with a related DP which is chosen rather ad hoc by removing coupling terms in the Hamiltonian; see, e.g., Ref. [26]. In contrast to inequality (34) the response of a system with a DP to a perturbation is (see the Appendix for a derivation)

$$|E_j - E_{\text{DP}}| \leq \varepsilon \|\hat{H}_1\|_2. \quad (43)$$

With the condition $E_{\text{DP}} = E_{\text{EP}}$ it is easy to show that the maximum splitting of the DP in Eq. (43) equals the maximum splitting of the EP in Eq. (34), cf. Fig. 2, if

$$\varepsilon_c \|\hat{H}_1\|_2 = \xi^{1/(n-1)}, \quad (44)$$

assuming that the perturbation is still small enough such that inequality (34) is valid. This rather elementary calculation reveals that the critical perturbation strength ε_c below which the maximum splitting of the EP exceeds that of the reference DP (which is here the nearest DP in matrix space) is determined by ξ .

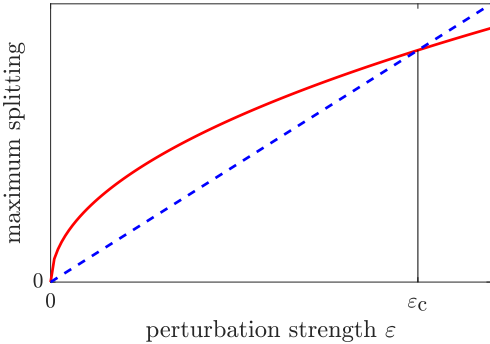


FIG. 2. Illustration of a comparison of the maximum splitting for an EP₂ (red solid curve) according to the inequality (34) and its nearest DP₂ (blue dashed line) according to the inequality (43) under a perturbation. The vertical line marks the critical perturbation strength ε_c below which the maximum splitting of the EP is larger.

V. PASSIVE SYSTEMS

In Ref. [34] it had been shown for the special cases $n = 2$ and $n = 3$ that there is an upper bound for the spectral response strength ξ in passive (no gain) systems. This upper bound limits the applicability of the given EP in particular in the sensing setting. In this section we derive an upper bound for the distance Δ for arbitrary n . With the inequality (42) this in turn generalizes the upper bound for ξ in Ref. [34].

For passive systems the Hermitian decay operator

$$\hat{\Gamma} := i(\hat{H}_0 - \hat{H}_0^\dagger) \quad (45)$$

is positive semidefinite; see, e.g., Refs. [55, 60]. With Eq. (28) we write

$$\hat{N} - \hat{N}^\dagger = -i(\hat{\Gamma} - \beta \mathbb{1}) \quad (46)$$

where we have introduced the real number

$$\beta := -2\text{Im } E_{\text{EP}}. \quad (47)$$

Considering the fact that both \hat{N} and \hat{N}^\dagger are traceless because of their nilpotency [49] one gets

$$\text{Tr } \hat{\Gamma} = n\beta. \quad (48)$$

For a positive semidefinite matrix $\text{Tr } \hat{\Gamma} \geq 0$ and hence $\beta \geq 0$. Taking the Frobenius norm on both sides of Eq. (46) gives

$$\|\hat{N} - \hat{N}^\dagger\|_{\text{F}} = \|\hat{\Gamma} - \beta \mathbb{1}\|_{\text{F}}. \quad (49)$$

In the following we assume that \hat{N} is a strictly upper triangular matrix. This can always be achieved by a unitary transformation of the Hamiltonian \hat{H}_{EP} which does not change the Frobenius norm; see Eq. (7). According to the Schur theorem (see, e.g., Ref. [59]), a unitary transformation exists that transforms the matrix \hat{N} defined in Eq. (28) to the sum of a diagonal matrix and a strictly upper triangular matrix. The former matrix is identical to zero because of the nilpotency

of \hat{N} . Obviously, if \hat{N} is a strictly upper triangular matrix then \hat{N}^\dagger is a strictly lower triangular matrix. With Eq. (10) it follows for the LHS of Eq. (49)

$$\|\hat{N} - \hat{N}^\dagger\|_{\text{F}} = \sqrt{2}\|\hat{N}\|_{\text{F}}. \quad (50)$$

With Eq. (5) and the Hermiticity of $\hat{\Gamma}$ we can rewrite Eq. (49) then as

$$\|\hat{N}\|_{\text{F}} = \frac{1}{\sqrt{2}} \sqrt{\text{Tr}[(\hat{\Gamma} - \beta \mathbb{1})^2]}. \quad (51)$$

The positive semidefiniteness of $\hat{\Gamma}$ restricts the maximum value of RHS of Eq. (51). It is attained when $\hat{\Gamma}$ is a rank-1 matrix. In this case, $\hat{\Gamma}$ has only one nonzero eigenvalue, which, according to Eq. (48), must be $n\beta$. With Eqs. (29) and (47) it follows the important result

$$\Delta(\hat{H}_{\text{EP}}) \leq \sqrt{2n(n-1)}|\text{Im } E_{\text{EP}}|. \quad (52)$$

This inequality valid for passive systems shows that the distance of a given EP to the set of DPs is bounded essentially by the decay rate at the EP. This bound can be transferred to the spectral response strength via inequality (42). It follows the next important result

$$\xi \leq \left(\sqrt{2n}|\text{Im } E_{\text{EP}}|\right)^{n-1}. \quad (53)$$

For $n = 2$ the bound in Ref. [34] for passive systems is recovered. For $n = 3$ a slightly lower bound is obtained here. This improved bound is consistent with the numerical data in Ref. [34]. It is to emphasize that Eq. (53) is valid for all $n \geq 2$. It is therefore a generalization of the results proven in Ref. [34].

Note that for small perturbation strength ε , inequality (53) together with the bound of the eigenvalue splittings (34) provide a much stronger statement than $\text{Im } E_j \leq 0$ which also has to be fulfilled in passive systems (including the perturbation).

The importance of inequality (53) becomes clear by remarking that $2|\text{Im } E_{\text{EP}}|$ is the linewidth of the spectral peak at the EP. Hence the upper bound for ξ in inequality (53) limits the resolvability of the frequency splittings under perturbation and therefore the performance of a sensor based on such an EP.

The result in inequality (53) has also significant consequences for the intensity response of passive systems to excitations. Consider the DP-analog of inequality (35) (see the Appendix for a short derivation),

$$\|\psi\|_2^{\text{DP}} = P \frac{1}{|\hbar\omega - E_{\text{DP}}|}. \quad (54)$$

We compare the response of the two kinds of degeneracies at resonance, i.e., at the EP [inequality (35)] with $\hbar\omega = \text{Re}(E_{\text{EP}})$ and at the DP [Eq. (54)] with $\hbar\omega = \text{Re}(E_{\text{DP}})$. Using inequality (53) we obtain

$$\frac{\|\psi\|_2^{\text{EP}}}{\|\psi\|_2^{\text{DP}}} \leq (2n)^{(n-1)/2}. \quad (55)$$

This inequality tells us how much an EP_n can enhance the intensity response to excitation in a passive system if compared to a reference DP_n. For $n = 2$ the maximal enhancement factor is 2 which is consistent with the findings in Ref. [61]. For $n = 3$ the maximal enhancement factor is 6.

VI. EXAMPLES

In this section we provide several examples to illustrate our approach.

A. Exceptional ring in wave-number space

Our first example stresses the difference between the commonly used parameter space and wave-number space on the one side and the matrix space discussed in this article on the other side. In Ref. [43] it has been shown that EPs can be created out of a Dirac point in a photonic crystal slab. The finite thickness of the slab introduces radiation losses which are dissimilar for the two involved dipole and quadrupole modes. The effective Hamiltonian to describe this situation is

$$\hat{H} = \begin{pmatrix} \omega_0 - i\alpha & g & 0 & 0 \\ g & \omega_0 + i\alpha & 0 & 0 \\ \kappa & 0 & \omega_0 - i\alpha & g \\ 0 & 0 & g & \omega_0 + i\alpha \end{pmatrix}, \quad (56)$$

where $\vec{k} = (k_x, k_y)$ is the two-dimensional wave vector, $\gamma \geq 0$ is the loss rate of the dipole mode (the loss of the quadrupole mode can be ignored), $\omega_0 > 0$ is the frequency of the unperturbed Dirac point, and $v_g > 0$ is the group velocity at the Dirac point. The eigenvalues of the Hamiltonian (56) are

$$\omega_{\pm} = \omega_0 - i\frac{\gamma}{2} \pm v_g \sqrt{|\vec{k}|^2 - k_c^2} \quad (57)$$

with the critical wave number $k_c := \gamma/(2v_g)$. In the absence of radiation ($\gamma = 0$), Eq. (57) describes the linear dispersion near the Dirac point, $\omega_{\pm} = \omega_0 \pm v_g |\vec{k}|$, the well-known Dirac cones.

If the loss rate γ is nonzero, even if it is very small, the system possesses an EP at $|\vec{k}| = k_c$. In the two-dimensional wave-number space (k_x, k_y) with all other parameters fixed this degeneracy therefore appears as a ring of EPs. In the three-dimensional parameter space $(\omega_0, v_g |\vec{k}|, \gamma)$ this degeneracy is the two-dimensional plane $v_g |\vec{k}| = \gamma/2$. Both the parameter space and the wave-number space are clearly different from the 2×2 -dimensional complex matrix space where the distance $\Delta(\hat{H}_{\text{EP}})$ of the EP to the set of DPs is defined. It is here calculated by inserting the Hamiltonian (56) at the EP and its eigenvalue $\omega_{\text{EP}} = \omega_0 - i\frac{\gamma}{2}$ via Eq. (28) into Eq. (29)

$$\Delta(\hat{H}_{\text{EP}}) = \gamma. \quad (58)$$

This result makes intuitively sense because it is here the loss that turns the DP into an EP. A small loss rate γ is sufficient but, according to Eq. (37), the spectral response strength

$\xi = \gamma$ is then also small. To enlarge the spectral response to perturbations one has to increase the loss in the photonic crystal slab by reducing the thickness of the slab which obviously has a limit.

Note that $\gamma = 2|\text{Im } \omega_{\text{EP}}|$, so that the inequality (53) for passive systems holds here with the equal sign.

B. Unidirectionally coupled pair of \mathcal{PT} -symmetric dimers

Our second example is a higher-order EP at which Δ and ξ are not equal. We consider a unidirectionally coupled pair of parity-time (\mathcal{PT})-symmetric dimers introduced in the context of hierarchical construction of higher-order EPs [62]. The Hamiltonian is

$$\hat{H} = \begin{pmatrix} \omega_0 - i\alpha & g & 0 & 0 \\ g & \omega_0 + i\alpha & 0 & 0 \\ \kappa & 0 & \omega_0 - i\alpha & g \\ 0 & 0 & g & \omega_0 + i\alpha \end{pmatrix}. \quad (59)$$

Each of the two 2×2 subblocks along the diagonal describes a \mathcal{PT} -symmetric dimer with real-valued frequency ω_0 , gain/loss coefficient $\alpha > 0$, and internal coupling coefficient $g > 0$. These two dimers are unidirectionally coupled with the strength $\kappa > 0$. This system can be realized experimentally by two evanescently coupled microrings each with two modes, one traveling clockwise and one counterclockwise [62]. One microring exhibits gain, the other one exhibits the equal amount of loss. The unidirectional coupling can be achieved by evanescently coupling the lossy microring to a semi-infinite waveguide with an end mirror [63]. This introduces a fully asymmetric backscattering [38] between the traveling waves in that microring.

For $\alpha = g$ the Hamiltonian possesses an EP₄ with real eigenvalue $\omega_{\text{EP}} = \omega_0$. Inserting this eigenvalue and the Hamiltonian (59) via Eq. (28) into Eq. (29) gives

$$\Delta(\hat{H}_{\text{EP}}) = \sqrt{8g^2 + \kappa^2}. \quad (60)$$

The Pythagoras-like appearance of $\Delta(\hat{H}_{\text{EP}})$ is in this case rather obvious. The experimental effort in realizing a significant $\Delta(\hat{H}_{\text{EP}})$ is based on implementing either a large internal coupling g or a large unidirectional coupling κ . For the spectral response strength (32) we get

$$\xi = 2g^2\kappa. \quad (61)$$

It can be easily verified that the inequality (42) is satisfied. Equation (61) tells us that large g or large κ is only a necessary but not a sufficient condition for getting a large response from the system at the EP. For the sufficient condition the product $g^2\kappa$ has to be large. The bound in inequality (53) does not apply since the system is not passive.

C. Coupling of optical modes with different angular momenta

The third example is a deformed microdisk cavity [64, 65]. The broad range of applications of deformed microcavities is

reviewed in [66]. For generating EPs in this kind of system a weak boundary deformation is sufficient [39, 40]. Such a boundary deformation can be expressed in polar coordinates as $r(\phi) = R + f(\phi)$ with the radius of the unperturbed microdisk R and the deformation function $|f(\phi)| \ll R$. We consider here only deformation functions that preserve a mirror-reflection symmetry. Moreover, we restrict ourselves to two modes. The mode with lower radiation losses is called mode 1. Its complex frequency is ω_1 and its azimuthal mode number is m . Mode 2 has the higher radiation losses, complex frequency ω_2 , and azimuthal mode number $p < m$. If the frequencies of the two modes are nearly degenerate, i.e., $\omega_1 \approx \omega_2$, a first-order perturbation theory can be applied leading to the effective non-Hermitian Hamiltonian [40]

$$\hat{H} = \begin{pmatrix} x_1 & 0 \\ 0 & x_2 \end{pmatrix} - x_1 \begin{pmatrix} A_{mm}^{e/o} & A_{mp}^{e/o} \\ A_{pm}^{e/o} & A_{pp}^{e/o} \end{pmatrix}. \quad (62)$$

The eigenvalues of this Hamiltonian are the frequencies of the two modes in the deformed microcavity. $x_i = \omega_i R/c$ are the dimensionless complex frequencies of the unperturbed modes and c is the speed of light in vacuum. The Fourier harmonics of the deformation function are given for the even and odd parity as

$$A_{pm}^e = \frac{\varepsilon_p}{\pi R} \int_0^\pi f(\phi) \cos(p\phi) \cos(m\phi) d\phi, \quad (63)$$

$$A_{pm}^o = \frac{\varepsilon_p}{\pi R} \int_0^\pi f(\phi) \sin(p\phi) \sin(m\phi) d\phi, \quad (64)$$

with $\varepsilon_p = 2$ if $p \neq 0$ and $\varepsilon_p = 1$ otherwise. Restricting to the relevant case $m, p > 0$ the matrix elements $A_{mp}^{e/o}$ and $A_{pm}^{e/o}$ are equal for fixed parity.

The Hamiltonian has an EP if

$$[x_1 - x_2 - x_1(A_{mm}^{e/o} - A_{pp}^{e/o})]^2 + 4x_1^2(A_{mp}^{e/o})^2 = 0. \quad (65)$$

The eigenvalue of the EP is

$$x_{EP} = \frac{x_1 + x_2}{2} - x_1 \frac{A_{mm}^{e/o} + A_{pp}^{e/o}}{2}. \quad (66)$$

Plugging this eigenvalue and the Hamiltonian (62) by means of Eq. (28) into Eq. (29) gives the distance to the set of DPs

$$\Delta(\hat{H}_{EP}) = 2|x_1 A_{mp}^{e/o}|. \quad (67)$$

Clearly, a weak deformation ($|A_{mp}^{e/o}| \ll 1$) implies a small distance $\Delta(\hat{H}_{EP})$. This in turn leads, according to Eq. (37), to a weak spectral response strength ξ to perturbations (e.g. induced by a nanoparticle close to the boundary of the microcavity). The response can therefore be enhanced if the deformation is increased. This, however, often leads to enhanced radiation losses [67]. Also note that if the deformation is too strong then the perturbation theory for weak boundary deformations is not valid any more.

D. Random Hamiltonians at EPs

Finally, we adopt the random-matrix approach invented in Ref. [34] to generate numerically a whole class of examples. To do so, we introduce the $n \times n$ matrix \hat{H}_{EP} having

an EP _{n} with eigenvalue E_{EP} via a similarity transformation $\hat{H}_{EP} = \hat{Q}\hat{J}\hat{Q}^{-1}$, with \hat{J} being an $n \times n$ matrix with an EP _{n} in Jordan normal form and \hat{Q} is an, in general nonunitary, $n \times n$ matrix consisting of complex random numbers with real and imaginary parts being drawn from a uniform distribution on the interval $[-1/2, 1/2]$. Clearly, \hat{H}_{EP} is not completely random, but nevertheless we refer to it as the “random Hamiltonian with an EP”.

To numerically confirm the inequality (42) we define the nonnegative quantity

$$x := \frac{(n-1)^{(n-1)/2}\xi}{\Delta(\hat{H}_{EP})^{n-1}}, \quad (68)$$

which should be less or equal unity. Figure 3 shows a histogram resulting from 10^7 realizations of random Hamiltonians for the case of an EP of order $n = 4$. It can be clearly seen that $x \leq 1$ and therefore the upper bound for the response strength ξ given by inequality (42) is fulfilled. The average and the maximal value of x are numerically determined to be ≈ 0.285 and ≈ 0.991 . The latter value indicates that the upper bound given by the RHS of inequality (42) is sharp. We observe this numerical indication of a sharp upper bound also for $n < 4$ but not for $n > 4$. For instance, for $n = 2, \dots, 6$ the maximal value of x [Eq. (68)] is 1, 1, 0.991, 0.902, and 0.736.

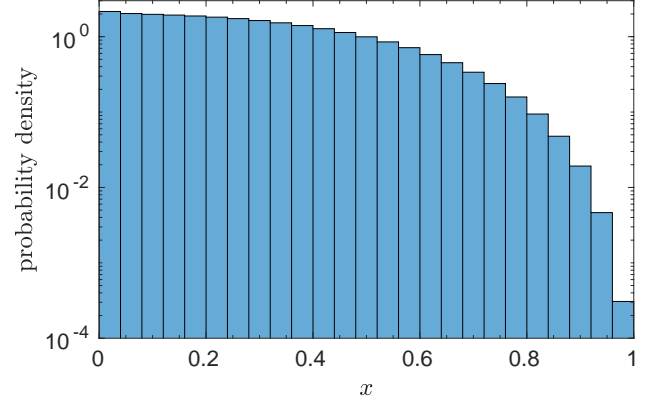


FIG. 3. Probability density function (notice the logarithmic scale) of the dimensionless number x defined in Eq. (68) computed from 10^7 realizations of random Hamiltonians having an EP₄ with eigenvalue $E_{EP} = -i0.5$.

To check the upper bound for the distance Δ [inequality (52)] and the spectral response strength ξ [inequality (53)] in passive systems, we consider the random Hamiltonians \hat{H}_{EP} with an EP _{n} for several values of n . We define the quantities

$$y := \frac{\Delta(\hat{H}_{EP})}{\sqrt{2n(n-1)|\text{Im } E_{EP}|}} \quad (69)$$

and

$$z := \frac{\xi}{(\sqrt{2n}|\text{Im } E_{EP}|)^{n-1}}, \quad (70)$$

which according to the inequalities (52) and (53) are less or equal unity. For each value of n , we select from 10^8 realizations of random Hamiltonians those that have a positive semidefinite decay operator $\hat{\Gamma}$ [Eq. (45)]. Figure 4 shows the resulting maximal values of y and z versus the order n . First, one can observe that $y_{\max}, z_{\max} \leq 1$. Hence the inequalities (52) and (53) are indeed fulfilled. Second, from $y_{\max} \geq z_{\max}$ we conclude that inequality (52) gives a sharper bound than inequality (53). This is understandable as the former bound results directly from the positive semidefinite-ness of $\hat{\Gamma}$, whereas the latter additionally requires the inequality (42).

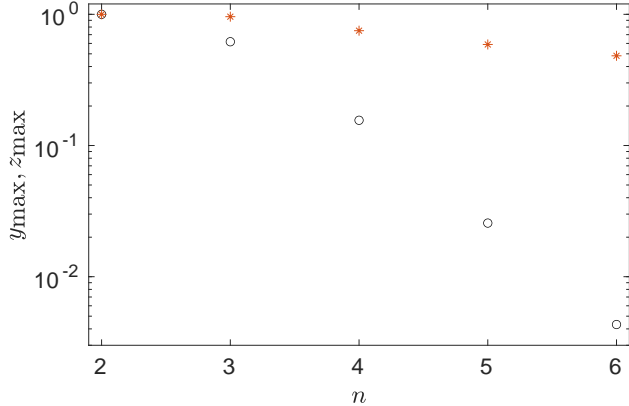


FIG. 4. Maximal values of the dimensionless distance y [Eq. (69), star symbols] and the dimensionless response strength z [Eq. (70), circle symbols] for passive systems as function of the order n of the EP; From 10^8 realizations (for each n) of random Hamiltonians having an EP _{n} with eigenvalue $E_{\text{EP}} = -i1.2$ those are selected that possess a positive semidefinite decay operator $\hat{\Gamma}$ [Eq. (45)]. Note the logarithmic scale on the vertical axis.

VII. SUMMARY

We have introduced the concept of the distance Δ of an $n \times n$ Hamiltonian to the set of DPs of order n in matrix space. This concept is mathematical in nature but it has physical relevance for non-Hermitian Hamiltonians with an EP. In this case, Δ is a vague measure of the experimental effort to create an EP out of a DP of the same order. Interestingly, Δ determines an upper bound for the spectral response strength ξ of the given system with the EP. This not only provides an easy way to estimate ξ , but, more importantly, it also reveals that the strategy of implementing experimentally an EP by slightly

modifying a DP results in an EP exhibiting only a weak response to perturbations. We have related the distance Δ to Henrici's departure from normality.

For passive systems we have derived an upper bound for the distance Δ . This bound engenders an upper bound for the spectral response strength ξ which constitutes an improvement and generalization of the bound for ξ in Ref. [34] to EPs of arbitrary order.

Analytical and numerical results for various physical examples have been presented which demonstrated the new insights in the physics of EPs provided by the concept introduced in this work.

ACKNOWLEDGMENTS

Valuable discussions with J. Kullig and R. El-Ganainy are acknowledged.

Appendix A: Spectral and intensity response at a DP

In this appendix we derive the spectral response to perturbations [inequality (43)] and the intensity response to excitations [Eq. (54)] for a system with a DP. To do so, we first consider the eigenvalue equation of the Hamiltonian (33)

$$(\hat{H}_{\text{DP}} + \varepsilon \hat{H}_1) |\psi_j\rangle = E_j |\psi_j\rangle \quad (\text{A1})$$

with $\hat{H}_0 = \hat{H}_{\text{DP}}$, eigenvalues E_j and eigenstates $|\psi_j\rangle$. With $\hat{H}_{\text{DP}} = E_{\text{DP}} \mathbb{1}$ we can write

$$\varepsilon \hat{H}_1 |\psi_j\rangle = (E_j - E_{\text{DP}}) |\psi_j\rangle. \quad (\text{A2})$$

Taking the vector 2-norm on both sides of this equation and using the normalization $\|\psi_j\|_2 = 1$ gives

$$\varepsilon \|\hat{H}_1 \psi_j\|_2 = |E_j - E_{\text{DP}}|. \quad (\text{A3})$$

Exploiting the compatibility of the matrix norm to the vector 2-norm (8) and again the normalization of the eigenstate gives inequality (43).

Next, we quickly derive the intensity response for $\hat{H} = \hat{H}_{\text{DP}} = E_{\text{DP}} \mathbb{1}$ by solving Eq. (36) with the ansatz $|\psi\rangle \propto e^{-i\omega t}$ to yield

$$|\psi\rangle = (E \mathbb{1} - E_{\text{DP}} \mathbb{1})^{-1} e^{-i\omega t} P |p\rangle \quad (\text{A4})$$

with excitation energy $E = \hbar\omega$. Taking the vector 2-norm on both sides of this equation and using the normalization $\|p\|_2 = 1$ gives Eq. (54).

[1] M.-A. Miri and A. Alù, Exceptional points in optics and photonics, *Science* **363**, eaar7709 (2019).
[2] S. K. Özdemir, S. Rotter, F. Nori, and L. Yang, Parity-time symmetry and exceptional points in photonics, *Nat. Materials* **18**, 783 (2019).
[3] T. Kato, *Perturbation Theory for Linear Operators* (Springer, New York, 1966).

[4] W. D. Heiss, Repulsion of resonance states and exceptional points, *Phys. Rev. E* **61**, 929 (2000).

[5] M. V. Berry, Physics of nonhermitian degeneracies, *Czech. J. Phys.* **54**, 1039 (2004).

[6] W. D. Heiss, Exceptional points of non-Hermitian operators, *J. Phys. A: Math. Gen.* **37**, 2455 (2004).

[7] M. V. Berry and M. Wilkinson, Diabolic points in the spectra of triangles, *Proc. R. Soc. Lond. A.* **392**, 15 (1984).

[8] C. Dembowski, H.-D. Gräf, H. L. Harney, A. Heine, W. D. Heiss, H. Rehfeld, and A. Richter, Experimental Observation of the Topological Structure of Exceptional Points, *Phys. Rev. Lett.* **86**, 787 (2001).

[9] C. Dembowski, B. Dietz, H.-D. Gräf, H. L. Harney, A. Heine, W. D. Heiss, and A. Richter, Encircling an exceptional point, *Phys. Rev. E* **69**, 056216 (2004).

[10] B. Dietz, T. Friedrich, J. Metz, M. Miski-Oglu, A. Richter, F. Schäfer, and C. A. Stafford, Rabi oscillations at exceptional points in microwave billiards, *Phys. Rev. E* **75**, 027201 (2007).

[11] S.-B. Lee, J. Yang, S. Moon, S.-Y. Lee, J.-B. Shim, S. W. Kim, J.-H. Lee, and K. An, Observation of an Exceptional Point in a Chaotic Optical Microcavity, *Phys. Rev. Lett.* **103**, 134101 (2009).

[12] B. Peng, S. K. Özdemir, F. Lei, F. Monfi, M. Gianfreda, G. L. Long, S. Fan, F. Nori, C. M. Bender, and L. Yang, Parity-time-symmetric whispering-gallery microcavities, *Nature Physics* **10**, 394 (2014).

[13] B. Peng, S. K. Özdemir, M. Liertzer, W. Chen, J. Kramer, H. Yilmaz, J. Wiersig, S. Rotter, and L. Yang, Chiral modes and directional lasing at exceptional points, *Proc. Natl. Acad. Sci. USA* **113**, 6845 (2016).

[14] S. Richter, H.-G. Zirnstein, J. Zúñiga-Pérez, E. Krüger, C. Deparis, L. Trefflich, C. Sturm, B. Rosenow, M. Grundmann, and R. Schmidt-Grund, Voigt Exceptional Points in an Anisotropic ZnO-Based Planar Microcavity: Square-Root Topology, Polarization Vortices, and Circularity, *Phys. Rev. Lett.* **123**, 227401 (2019).

[15] Y. Choi, S. Kang, S. Lim, W. Kim, J.-R. Kim, J.-H. Lee, and K. An, Quasieigenstate Coalescence in an Atom-Cavity Quantum Composite, *Phys. Rev. Lett.* **104**, 153601 (2010).

[16] A. Regensburger, C. Bersch, M.-A. Miri, G. Onishchukov, D. N. Christodoulides, and U. Peschel, Parity-time synthetic photonic lattices, *Nature (London)* **488**, 167–171 (2012).

[17] T. Gao, E. Estrecho, K. Y. Bliokh, T. C. H. Liev, M. D. Fraser, S. Brodbeck, K. M., C. Schneider, S. Höfling, Y. Yamamoto, F. Nori, Y. S. Kivshar, A. G. Truscott, R. G. Dall, and E. A. Ostrovskaya, Observation of non-Hermitian degeneracies in a chaotic exciton-polariton billiard, *Nature (London)* **526**, 554 (2015).

[18] Y. Shin, H. Kwak, S. Moon, S.-B. Lee, J. Yang, and K. An, Observation of an exceptional point in a two-dimensional ultrasonic cavity of concentric circular shells, *Sci. Rep.* **6**, 38826 (2016).

[19] S. Wang, B. Hou, W. Lu, Y. Chen, Z. Q. Zhang, and C. T. Chan, Arbitrary order exceptional point induced by photonic spin–orbit interaction in coupled resonators, *Nat. Commun.* **10**, 832 (2019).

[20] P. Miao, Z. Zhang, J. Sun, W. Walasik, S. Longhi, N. M. Litchinitser, and L. Feng, Orbital angular momentum microlaser, *Science* **353**, 464 (2016).

[21] S. Richter, T. Michalsky, C. Sturm, B. Rosenow, M. Grundmann, and R. Schmidt-Grund, Exceptional points in anisotropic planar microcavities, *Phys. Rev. A* **95**, 023836 (2017).

[22] H. Xu, D. Mason, L. Jiang, and J. G. E. Harris, Topological energy transfer in an optomechanical system with exceptional points, *Nature (London)* **537**, 80 (2016).

[23] J. Doppler, A. A. Mailybaev, J. Böhm, U. Kuhl, A. Girschik, F. Libisch, T. J. Milburn, P. Rabl, N. Moiseyev, and S. Rotter, Dynamically encircling an exceptional point for asymmetric mode switching, *Nature (London)* **537**, 76 (2016).

[24] B. Peng, S. K. Özdemir, S. Rotter, H. Yilmaz, M. Liertzer, F. Monfi, C. M. Bender, F. Nori, and L. Yang, Loss-induced suppression and revival of lasing, *Science* **17**, 328 (2014).

[25] H. Hodaei, M.-A. Miri, M. Heinrich, D. Christodoulides, and M. Khajavikhan, Parity-time-symmetric microring lasers, *Science* **346**, 975 (2014).

[26] J. Wiersig, Enhancing the Sensitivity of Frequency and Energy Splitting Detection by Using Exceptional Points: Application to Microcavity Sensors for Single-Particle Detection, *Phys. Rev. Lett.* **112**, 203901 (2014).

[27] W. Chen, S. K. Özdemir, G. Zhao, J. Wiersig, and L. Yang, Exceptional points enhance sensing in an optical microcavity, *Nature (London)* **548**, 192 (2017).

[28] H. Hodaei, A. Hassan, S. Wittek, H. Garcia-Cracia, R. El-Ganainy, D. Christodoulides, and M. Khajavikhan, Enhanced sensitivity at higher-order exceptional points, *Nature (London)* **548**, 187 (2017).

[29] Z. Xiao, H. Li, T. Kottos, and A. Alù, Enhanced sensing and nondegraded thermal noise performance based on PT-symmetric electronic circuits with a sixth-order exceptional point, *Phys. Rev. Lett.* **123**, 213901 (2019).

[30] Y.-H. Lai, Y.-K. Lu, M.-G. Suh, Z. Yuan, and K. Vahala, Observation of the exceptional-point-enhanced Sagnac effect, *Nature (London)* **576**, 65 (2019).

[31] H. Wang, Y.-H. Lai, Z. Yuan, M.-G. Suh, and K. Vahala, Petermann-factor sensitivity limit near an exceptional point in a Brillouin ring laser gyroscope, *Nat. Commun.* **11**, 1610 (2020).

[32] R. Kononchuk, J. Cai, F. Ellis, R. Thevamaran, and T. Kottos, Enhanced signal-to-noise performance of EP-based electromechanical accelerometers, *arXiv:2201.13328* (2022).

[33] J. Wiersig, Review of exceptional point-based sensors, *Photonics Res.* **8**, 1457 (2020).

[34] J. Wiersig, Potential response strengths of open systems at exceptional points, *Phys. Rev. Res.* **4**, 023121 (2022).

[35] F. Keck, H. J. Korsch, and S. Moessmann, Unfolding a diabolic point: a generalized crossing scenario, *J. Phys. A: Math. Gen.* **36**, 2125 (2003).

[36] H. Wang, K. L. Zhang, and Z. Song, Transition from degeneracy to coalescence: Theorem and applications, *Phys. Rev. B* **104**, 245406 (2020).

[37] J. Wiersig, Structure of whispering-gallery modes in optical microdisks perturbed by nanoparticles, *Phys. Rev. A* **84**, 063828 (2011).

[38] J. Wiersig, Non-Hermitian effects due to asymmetric backscattering of light in whispering-gallery microcavities, in *Parity-time Symmetry and Its Applications*, edited by D. Christodoulides and J. Yang (Springer, Singapore, 2018) pp. 155–184.

[39] C.-H. Yi, J. Kullig, and J. Wiersig, Pair of exceptional points in a microdisk cavity under an extremely weak deformation, *Phys. Rev. Lett.* **120**, 093902 (2018).

[40] J. Kullig, C.-H. Yi, and J. Wiersig, Exceptional points by coupling of modes with different angular momenta in deformed microdisks: A perturbative analysis, *Phys. Rev. A* **98**, 023851 (2018).

[41] J. Feilhauer, A. Schumer, J. Doppler, A. A. Mailybaev, J. Böhm, U. Kuhl, N. Moiseyev, and S. Rotter, Encircling exceptional points as a non-Hermitian extension of rapid adiabatic passage, *Phys. Rev. A* **102**, 040201(R) (2020).

[42] R. Schäfer, J. C. Budich, and D. J. Luitz, Symmetry protected exceptional points of interacting fermions, [arXiv:2204.05340](https://arxiv.org/abs/2204.05340) (2022).

[43] B. Zheng, C. W. Hsu, Y. Igarashi, L. Lu, I. Kaminer, A. Pick, S.-L. Chua, J. D. Joannopoulos, and M. Soljačić, Spawning rings of exceptional points out of Dirac cones, *Nature (London)* **525**, 354 (2015).

[44] Z. Lin, A. Pick, M. Loncar, and A. W. Rodriguez, Enhanced spontaneous emission at third-order Dirac exceptional points in inverse-designed photonic crystals, *Phys. Rev. Lett.* **117**, 107402 (2016).

[45] H. Zhou, C. Peng, Y. Yoon, C. W. Hsu, K. A. Nelson, L. Fu, J. D. Joannopoulos, M. Soljačić, and B. Zhen, Observation of bulk Fermi arc and polarization half charge from paired exceptional points, *Nature (London)* **359**, 1009 (2018).

[46] A. Cerjan, S. Huang, M. Wang, K. P. Chen, Y. Chong, and M. C. Rechtsman, Experimental realization of a Weyl exceptional ring, *Nat. Photonics* **13**, 623 (2019).

[47] A. A. Zyuzin and P. Simon, Disorder-induced exceptional points and nodal lines in Dirac superconductors, *Phys. Rev. B* **99**, 165145 (2019).

[48] R. Rausch, R. Peter, and T. Yoshida, Exceptional points in the one-dimensional Hubbard model, *New J. Phys.* **23**, 013011 (2021).

[49] R. A. Horn and C. R. Johnson, *Matrix Analysis* (Cambridge University Press, Cambridge, 2013).

[50] J. E. Gentle, *Matrix Algebra: Theory, Computations, and Applications in Statistics* (Springer, Switzerland, 2017).

[51] N. J. Higham, Matrix nearness problems and applications, in *Applications of Matrix Theory*, edited by M. J. C. Gover and S. Barnett (Oxford University Press, Berlin, 1989).

[52] J. W. Demmel, On condition numbers and the distance to the nearest ill-posed problem, *Numer. Math.* **51**, 251 (1987).

[53] J. T. Chalker and B. Mehlig, Eigenvector statistics in non-Hermitian random matrix ensembles, *Phys. Rev. Lett.* **81**, 3367 (1998).

[54] Y. V. Fyodorov and B. Mehlig, Statistics of resonances and nonorthogonal eigenfunctions in a model for single-channel chaotic scattering, *Phys. Rev. E* **66**, 045202(R) (2002).

[55] J. Wiersig, Nonorthogonality constraints in open quantum and wave systems, *Phys. Rev. Res.* **1**, 033182 (2019).

[56] H. Schomerus, Excess quantum noise due to mode nonorthogonality in dielectric microresonators, *Phys. Rev. A* **79**, 061801(R) (2009).

[57] H. Schomerus, Random matrix approaches to open quantum systems, in *Stochastic Processes and Random Matrices*, Les Houches Summer School Lectures, Vol. 104, edited by G. Schehr *et al.* (North Holland, Amsterdam, 2017).

[58] P. Henrici, Bounds for iterates, inverses, spectral variation and fields of values of non-normal matrices, *Numerische Mathematik* **4**, 24 (1962).

[59] M. I. Gil, *Operator Functions and Localization of Spectra*, Lecture Notes in Mathematics, Vol. 1830 (Springer, Berlin, 2003).

[60] J. Wiersig, Sensors operating at exceptional points: General theory, *Phys. Rev. A* **93**, 033809 (2016).

[61] S. Sunada, Enhanced response of non-Hermitian photonic systems near exceptional points, *Phys. Rev. A* **97**, 043804 (2018).

[62] Q. Zhong, J. Kou, S. K. Özdemir, and R. El-Ganainy, Hierarchical construction of higher-order exceptional points, *Phys. Rev. Lett.* **125**, 203602 (2020).

[63] Q. Zhong, S. K. Özdemir, A. Eisfeld, A. Metelmann, and R. El-Ganainy, Exceptional points-based optical amplifiers, *Phys. Rev. Appl.* **13**, 014070 (2020).

[64] J. U. Nöckel and A. D. Stone, Ray and wave chaos in asymmetric resonant optical cavities, *Nature (London)* **385**, 45 (1997).

[65] C. Gmachl, F. Capasso, E. E. Narimanov, J. U. Nöckel, A. D. Stone, J. Faist, D. L. Sivco, and A. Y. Cho, High-Power Directional Emission from Microlasers with Chaotic Resonators, *Science* **280**, 1556 (1998).

[66] H. Cao and J. Wiersig, Dielectric microcavities: Model systems for wave chaos and non-Hermitian physics, *Rev. Mod. Phys.* **87**, 61 (2015).

[67] J. U. Nöckel, A. D. Stone, and R. K. Chang, *Q* spoiling and directionality in deformed ring cavities, *Opt. Lett.* **19**, 1693 (1994).